Received: 31 December 2021 | Accepted: 14 April 2022

DOI: 10.1111/1365-2435.14066

Functional Ecology | BRITISH ECOLOGICAL SOCIETY

RESEARCH ARTICLE

Temporal variation in stomatal sensitivity to vapour pressure deficit in western riparian forests

Jessica S. Guo[1] | Susan E. Bush[2] | Kevin R. Hultine[3]

[1]Arizona Experiment Station, College of Agriculture and Life Sciences, University of Arizona, Tucson, AZ, USA

[2]Department of Biological Sciences, University of Utah, Salt Lake City, UT, USA

[3]Department of Research, Conservation, and Collections, Desert Botanical Garden, Phoenix, AZ, USA

Correspondence
Jessica S. Guo
Email: jessicaguo@email.arizona.edu

Funding information
National Institute of Food and Agriculture, Grant/Award Number: 2015-67013-12138; National Science Foundation, Grant/Award Number: 1340856

Handling Editor: Tamir Klein

Abstract

1. Increasing atmospheric vapour pressure deficit (*D*) can influence plant water and carbon uptake. However, growing season variation in stomatal responses to *D* among tree taxa has not been thoroughly quantified and therefore has not been well-characterized in stomatal regulation models.
2. Using sap flux data from nine riparian species spanning a 600-m elevation gradient in semi-arid northern Utah, USA, we fit a time-varying empirical model of stomatal conductance to *D* in a hierarchical Bayesian framework. The reference conductance (G_{ref}, conductance at $D = 1$ kPa) term was modelled as a function of cumulative growing season *D*, which varied with site elevation.
3. Seven species exhibited G_{ref} that varied significantly with cumulative growing season *D*, but the direction was not consistent among species. Two low-elevation ring-porous species, the invasive *Tamarix ramosissima* and *Elaeagnus angustifolia*, exhibited significantly positive correlation between G_{ref} and cumulative *D*, such that standardized stomatal sensitivity (*S*) decreased during the season. Despite lower *D* at the mid- and high-elevation sites, five diffuse-porous native species exhibited progressively increasing sensitivity to *D* during the growing season.
4. Stomatal strategies exhibit seasonal trends that vary by environmental conditions (*D*) and functional traits (wood anatomy), which complicates the prediction of plant hydraulic function under increasing atmospheric drought. In the increasingly arid western United States, the progressively less sensitive stomatal behaviour of invasive taxa may hasten their dominance in riparian forests.

KEYWORDS
hydraulic regulation, iso/anisohydry, ring/diffuse porous, riparian tree species, stomatal behaviour, wood anatomy

Jessica S. Guo and Susan E. Bush—Co-first authors.

No permits were needed to conduct the original fieldwork.

1 | INTRODUCTION

Rising land surface temperature is facilitating global increases in atmospheric vapour pressure deficit (*D*), particularly in arid regions such as sub-Saharan Africa and the southwestern United States and northern Mexico (Grossiord et al., 2020; Hatfield & Prueger, 2015). Consequently, quantifying how changes in *D* impact photosynthetic gas exchange and subsequent carbon and water cycles at local to global scales is a priority among scientists across many disciplines (Novick et al., 2016). Rising vapour pressure deficit, and more specifically, rising leaf-to-air vapour pressure deficit, causes vascular plants to close their stomata (Brodribb & McAdam, 2011), resulting in reduced stomatal conductance (G_s). Reductions in G_s could prevent critical water potentials that would otherwise induce hydraulic failure, cease delivery of xylem water to the canopy and thereby reduce carbon assimilation (Sperry et al., 2002). However, an inevitable trade-off with stomatal closure is the reduction in carbon uptake that would otherwise support productivity, reproduction, maintenance respiration and the synthesis of secondary metabolites for defence. Thus, rising *D* could have profound impacts on vegetation cover, net primary productivity and ecosystem carbon sequestration in the coming decades (Novick et al., 2016; Yuan et al., 2019).

Stomatal sensitivity to *D* is highly variable among terrestrial plants, and consequently, rising *D* should have wide-ranging impacts across plant taxa (McNaughton & Jarvis, 1991; Ogle et al., 2012; Oren, Sperry, et al., 1999; Whitehead & Jarvis, 1981). One well-accepted empirical model utilizes the linear relationship between G_s and log(*D*) (Oren, Sperry, et al., 1999), such that the magnitude of the slope (*m*) represents stomatal sensitivity to *D* and the intercept parameter G_{ref} indicates the reference conductance when $D = 1$ kPa. Stem sap flux measurements of over 30 species showed a consistent relationship between G_s at low *D* (i.e. G_{ref}) and sensitivity to *D* (i.e. *m*) such that plant taxa with a high G_{ref} are generally more sensitive to increasing *D* (Oren, Sperry, et al., 1999). Furthermore, the index of standardized stomatal sensitivity (S: $-m/G_{ref}$) tends to converge at 0.6 in a wide range of mesic species, though *S* is often considerably lower for arid-adapted species (Oren, Sperry, et al., 1999). The consistently higher value of *S* among mesic species suggests greater stomatal sensitivity to *D*, whereby leaf water potential (Ψ_{leaf}) is regulated above a threshold and consistent with an isohydric hydraulic strategy. Conversely, lower values of *S* in arid-adapted plants indicate lower stomatal sensitivity that permits declines in Ψ_{leaf}, reflecting a more anisohydric hydraulic strategy (Ogle et al., 2012). Given contrasts in stomatal sensitivity to *D* among functional groups, patterns of *S* should also reflect contrasts in plant hydraulic function [e.g. maximum xylem hydraulic conductivity (k_{max}) and drought-induced xylem cavitation vulnerability], leaf and wood economic traits [e.g. leaf longevity (Mediavilla & Escudero, 2003) and wood density (Fu & Meinzer, 2018)] and wood anatomy (Klein, 2014).

One potential pitfall for classifying plant taxa into discrete hydraulic categories is that stomatal regulation may vary seasonally in response to changes in soil moisture, *D* or other environmental conditions that impact plant growth and allometry (Guo et al., 2020). In most temperate regions, the growing season is often punctuated by periods of high aridity and subsequently high *D* that can lead to reductions in whole-plant conductivity (Domec et al., 2009), even in species that tightly regulate Ψ_{leaf}. Likewise, some angiosperms experience a progressive weakening of xylem pit-pore membranes that increase vulnerability to xylem cavitation over the growing season (Hacke et al., 2001). Finally, the timing and sensitivity of root growth, xylem growth and canopy expansion can alter the balance of water supply and demand (Doughty & Goulden, 2008). However, the extent to which changes in plant hydraulic function and allometry over the growing season impacts stomatal sensitivity is an open question. On one hand, seasonal reductions in k_{max} or changes in whole-plant allometry should correspond with changes in maximum G_s (e.g. G_{ref}), in which case *m* could also vary (Aspinwall et al., 2011; Domec et al., 2009). Alternatively, xylem cavitation fatigue spurred by weakening pit-pore membranes (Hacke et al., 2001) could substantially increase sensitivity of G_s to *D* independent of impacts on G_{ref}. Changes in stomatal sensitivity could also be triggered by changes in leaf hormone concentrations, particularly abscisic acid (McAdam et al., 2016; Pantin et al., 2013), source–sink relationships related to growth and reproduction (Hultine et al., 2013), photosynthetic capacity (Katul et al., 2003; Sperry et al., 2017) and foliage loss caused by episodic disturbance (Ewers et al., 2007; Oren, Phillips, et al., 1999; Schäfer, 2011).

Riparian ecosystems in the arid western United States are in many ways ideal for evaluating stomatal sensitivity to *D* across a diverse group of tree taxa. First, western riparian trees are generally not subject to soil water deficits due to the presence of shallow groundwater tables. Therefore, stomatal conductance is generally not constrained by limited soil moisture. Second, arid regions of the west are characterized by periods of low humidity and high solar irradiance, such that *D* reaches levels that constrain G_s but photosynthetically active radiation does not. Third, global circulation models indicate that the arid west will experience some of the most profound increases in aridity in the coming decades, resulting in more frequent and intense heat waves that will spur episodic spikes in *D* (Grossiord et al., 2020). Finally, riparian tree taxa are recognized as foundation species that provide critical habitat for numerous threatened and endangered plant and animal species in a region where habitat suitability is limited by aridity (Hultine et al., 2020; Whitham et al., 2006). Therefore, riparian trees can serve as model taxa to evaluate stomatal sensitivity to *D*.

In this paper, we synthesized sap flux-scaled stomatal conductance and leaf water potential, collected from nine dominant riparian tree species in the Great Basin in northern Utah, USA, occurring across broad gradients in elevation and growing season *D*. We asked two related questions. First, to what extent does standardized sensitivity to *D* (*S*) change over the course of the growing season. And second, are growing season patterns of *S* consistent across taxa, or do they correspond to differences in exposure to cumulative *D* over the growing season? The following two alternative hypotheses were tested: 1. Standardized stomatal sensitivity (*S*) to *D* increases similarly in all species, reflecting a progressive decrease in G_{ref} relative to

m. 2. Growing season changes in *S* instead vary among species, with species exposed to greater cumulative *D* experiencing increased stomatal sensitivity.

Despite recently published global syntheses on sap flux-scaled stomatal conductance (Flo et al., 2021; Poyatos et al., 2021), to our knowledge, this study is among the first to exclusively investigate how stomatal sensitivity to *D* changes over the growing season across a broad range of taxa where other limiting factors such as soil moisture deficits and sunlight are largely absent. Additionally, this study advances our understanding of how ecologically important riparian tree species respond to seasonal changes in atmospheric aridity in a region where increases in aridity are expected over the next several decades.

2 | MATERIALS AND METHODS

2.1 | Study sites and tree species

Four riparian forest sites were selected for tree sap flux studies within the Great Salt Lake drainage basin of northern Utah, USA, spanning an elevational gradient of 1,314–1,900 m (Figure 1, Table 1). A total of nine tree species (Table 1) were instrumented to record sap flow dynamics and site-level environmental variables from June to September 2004. Predawn and midday water potential data were also collected monthly.

The lowest elevation site (labelled Jordan) was located in a riparian area along the Jordan River in Salt Lake Valley, Utah, USA (40°34′30″N; 111°55′03″W; 1,314 m elevation). The study site was in an unmanaged area located directly adjacent to the Jordan River, with a tree canopy largely comprised of mature non-native *Elaeagnus angustifolia* L. (n = 10), native *Populus fremontii* Watts. (n = 9) and non-native *Tamarix* (n = 9), a hybrid mixture between *T. ramosissima* and *T. chinensis* (Gaskin & Kazmer, 2009), but hereafter referred to as *T. ramosissima*. An on-site piezometer never recorded depth to groundwater exceeding 1 m. Sap flux data for *P. fremontii* and *E. angustifolia* at this site were originally published by Hultine and Bush (2011), while data for co-occurring *T. ramosissima* are unpublished. All of the selected trees occurred within the lowest terrace of the riparian area.

The remaining three sap flux installation sites were located within the Red Butte Canyon Research Natural Area (RBC) east of Salt Lake City, Utah, USA. The lowest site in RBC (labelled Reservoir) was located near the inlet of an artificial reservoir constructed near the mouth of the canyon (40°46′45.01″N, 111°48′29.73″W, 1,640 m elevation) with a riparian tree canopy that comprised of mature *Populus* hybrids (n = 7), a mixture between native *P. angustifolia* and *P. fremontii* and mature *Salix* hybrids (n = 9), likely comprising multiple *Salix* spp. Sap flux data for *Populus* and *Salix* hybrids at this site were originally published by Hultine, Bush, and Ehleringer (2010). All of the selected trees occurred along the bank of the reservoir that was actively managed to minimize fluctuations in stage height.

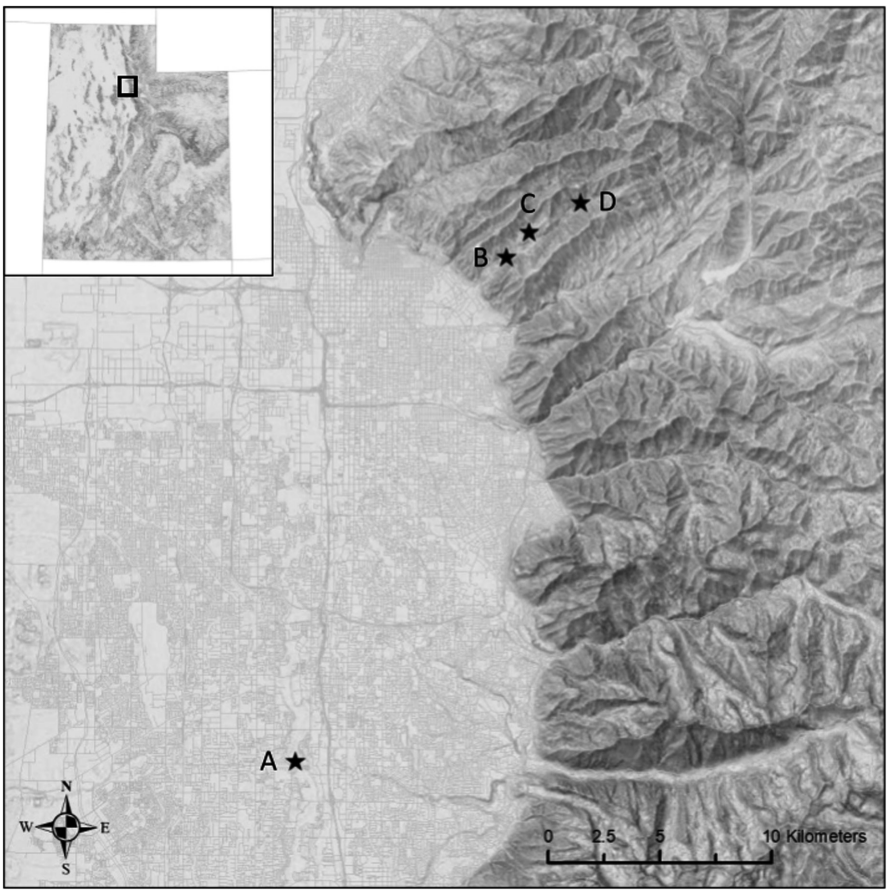

FIGURE 1 Map showing four study sites of (a) Jordan (1,314 m), (b) Reservoir (1,640 m), (c) Parley's (1,820 m) and (d) Upper (1,900 m) across an elevation gradient in northern Utah, USA

TABLE 1 Site and species description. N_{ind} denotes the sample size of individual trees instrumented with sap flow sensors, N_{obs} denotes the sample size of daily observations measured for each species and DBH indicates the range in DBH across individuals

Site name	Elevation (m)	Lat	Lon	Species	N_{ind}	N_{obs}	DBH (cm)	Wood anatomy	Status
Jordan	1,314	40°34′30″N	111°55′03″W	[a]*Populus fremontii*	9	303	(13.7, 57.6)	Diffuse-porous	Native
				[d]*Tamarix ramosissima*	9	307	(6.7, 11.1)	Ring-porous	Invasive
				[a]*Elaeagnus angustifolia*	10	401	(10.8, 22.6)	Ring-porous	Invasive
Reservoir	1,640	40°460′45″N	110°48′30″W	[b]*Populus* hybrid	7	185	(16.25, 33.5)	Diffuse-porous	Native
				[b]*Salix* hybrid	9	318	(10, 21.75)	Diffuse-porous	Native
Parley's	1,820	40°790′N	111°79′W	[c]*Acer negundo*	16	470	(5.5, 46.9)	Diffuse-porous	Native
Upper	1,900	40°800′N	111°77′W	[c]*Acer grandidentatum*	9	259	(6.9, 26.7)	Diffuse-porous	Native
				[c]*Betula occidentalis*	7	182	(7.7, 14.2)	Diffuse-porous	Native
				[c]*Populus angustifolia*	6	176	(10.5, 23.5)	Diffuse-porous	Native

[a]Hultine and Bush (2011).
[b]Hultine, Bush, and Ehleringer (2010).
[c]Hultine et al. (2007).
[d]Previously unpublished.

The mid-elevation site (labelled Parley's) in RBC was located in a 4.3 ha meadow in Parley's Fork approximately 200 m above the confluence with the main channel (40°47′20.84″N, 111°47′46.84″W, 1,820 m elevation). The overstorey at this site was comprised almost exclusively of mature *Acer negundo* Sarg. ($n = 16$), which lined a small perennial creek that flowed through the meadow. Sap flux data for *A. negundo* at this site were originally published by Hultine et al. (2007).

The upper elevation site (labelled Upper) was located along the main channel of RBC (40°48′04.27″N, 111°46′09.31″W, 1,900 m elevation) with a riparian overstorey dominated by mixed age stands of *A. negundo*, *Acer grandidentatum* Nutt., *Betula occidentalis* Hook. and *Populus angustifolia* James. Sap flux data for *A. grandidentatum* ($n = 9$), *B. occidentalis* ($n = 7$) and *P. angustifolia* ($n = 6$) at this site were originally published by Hultine et al. (2007). All trees measured for sap flux occurred within the lowest terrace of the riparian area.

2.2 | Sap flow measurements

During the 2004 growing season, measurements of stem sap flow were made using Granier-type thermal dissipation probes (Granier, 1987), where the temperature difference between a heated and reference sensor pair is empirically related to sap flux density (J_s, $g\,m^{-2}\,s^{-1}$) according to the following:

$$J_s = a\left(\Delta T_m/\Delta T - 1\right)^b, \quad (1)$$

where ΔT is the temperature difference between the heated and reference sensors, ΔT_m is the temperature difference between the heated and reference sensors measured under zero-flow conditions (Granier, 1987), and a and b are empirical coefficients. For the diffuse-porous species, a and b were 119 and 1.231, respectively, as originally reported by Granier (1987). Species-specific independent calibration determined from controlled experiments were applied to the ring-porous *T. ramosissima* (Hultine, Nagler, et al., 2010) and *E. angustifolia*, (Bush et al., 2010). For ΔT_m, we assumed zero-flow conditions only during night-time hours when vapour pressure deficit was at or near zero.

Each tree was instrumented with two 20-mm length, stainless steel probes, separated vertically by ~15 cm. The azimuth direction of sensor-pair placement around the bole of the trees was randomized. From measurements made every 30 s, 30-min means were logged at the Jordan site (CR23X; Campbell Scientific) and 15-min means were logged at the remaining sites (CR10X; Campbell Scientific).

2.3 | Meteorological variables and calculations

Air temperature (T, °C) and relative humidity (RH, %) were measured at each study site using temperature and relative humidity probes in combination with an aspirated radiation shield (HMP45C; Vaisala). Micrometeorological stations were co-located with study trees and measurements were stored at 15- or 30-min intervals and combined to calculate vapour pressure deficit (D, kPa).

We developed a metric of cumulative exposure to daily maximum D, akin to growing degree days (McMaster & Wilhelm, 1997):

$$CDE_n = \sum_1^n \begin{cases} D_{max_n} - D_{ref}, & D_{max_n} > D_{ref} \\ 0, & D_{max_n} \le D_{ref} \end{cases}, \quad (2)$$

where D_{max} is the daily maximum D, D_{ref} is the reference value of 1 kPa and n represents the day of year. Calculation of cumulative D exposure (CDE, kPa · days) required continuous daily records of D, which were not available at each site due to occasional power failure. Therefore, D_{max} at the four sites were gap-filled from the nearby (≤14.5 km) Olympus Hills weather station (1,512 m elevation) in the MesoWest network (Horel et al., 2002); daily maximum

D at Olympus Hills was calculated from 15-min records of T and RH. R^2 between D_{max} from each site and D_{max} at Olympus Hills ranged from 0.82 to 0.95. CDE was calculated as the cumulative sum of gap-filled D_{max} exceeding 1 kPa beginning with 1 January 2004, thereby accounting for both D extremes and the extent of time.

2.4 | Conductance calculations

Daily canopy conductance (G_c) was calculated from mean daytime sap flux (J_s, from 07:00 to 20:00) by a simplified form of the Penman–Monteith equation (Monteith & Unsworth, 1990):

$$G_c = \frac{\gamma \lambda}{\rho c_p D} \bullet J_s, \quad (3)$$

where γ is the psychrometric constant (kPa/K), λ is latent heat of vaporization (J/kg), ρ is density of moist air (kg/m ^{3}) and c_p is the specific heat of air at constant pressure (J kg^{-1} K^{-1}).

While Equation 3 typically includes the leaf area to sapwood area ratio, leaf area was not available for all species. Thus, G_c was reported on sapwood area basis, rather than a leaf area basis. Likewise, because measurements of leaf area and leaf area index were unavailable for most species, G_c was assumed to approximate G_s. Although canopies of broadleaved trees can decouple from the atmosphere and result in underestimates of sap flux-scaled G_s, canopy decoupling coefficients collected for *A. negundo* at the Parley's site were generally quite low, ranging from 0.09 to 0.25 (Hultine et al., 2008). A more recent study conducted on *P. fremontii* trees in Arizona reported decoupling coefficients that ranged from 0.03 to 0.05 over the growing season (Blasini et al., 2022). As a consequence, G_c of *A. negundo* and *P. fremontii* closely approximated G_s. Likewise, canopy decoupling in trees with narrow scale-like leaves such as *T. ramosissima* is generally insignificant. We are therefore confident that sap flux-scaled G_c reasonably approximated G_s at all field locations.

2.5 | Water potential

Water potential data were obtained monthly (see Figure S1 for dates) during the sap flux instrumentation period using a Scholander-type pressure chamber (PMS Instruments). Except for *A. negundo* ($n = 23$), five individuals of each species were sampled at each site. Predawn measurements (Ψ_{pd}) were made between 02:00 and 05:00; midday measurements (Ψ_{md}) were made between 11:00 and 14:00 on leaves obtained from sunlit portions of the tree canopy. Height of sample collection varied depending on species architecture but was consistent within species and across sampling dates. For each measurement, a small branch segment was collected using a pole pruner and immediately placed in a bag containing a wet paper towel. The sample was transported to the pressure chamber within 5 min, where a razor blade was used to excise one leaf for measurement.

2.6 | Model description

Preliminary data exploration indicated that G_{ref} (intercept) values change across the growing season for multiple species (Figure S2). Therefore, we specified a hierarchical Bayesian model to relate canopy conductance (G_c) to two covariates (D_{max}, CDE), which allowed for time-varying estimates of G_{ref} and stomatal sensitivity. The data model describes the likelihood of the observed G_c, which was normally distributed for each observation i ($i = 1, 2, \ldots 2{,}579$):

$$G_c \sim \text{Normal}(\bar{g}_i, \sigma^2) \quad (4)$$

where $\bar{g}_i$ is the predicted or mean conductance and the variance σ^2 represents the uncertainty in observed G_c. The mean conductance was modelled:

$$\bar{g}_i = G_{ref_i} - m_{t(i)} \bullet \log(D_{max_i}), \quad (5)$$

where G_{ref} is the reference conductance when D_{max} is 1 kPa, m is the sensitivity of conductance to log(D_{max}) and $t(i)$ indicates tree t associated with observation i. To allow for time-varying estimates of the intercept, G_{ref} was indexed by i and modelled as a linear function of CDE:

$$G_{ref_i} = \alpha_{t(i)} + \beta_{t(i)} \bullet \text{CDE}_i, \quad (6)$$

such that α represents G_{ref} at the initiation of CDE accumulation and β represents the effect of CDE on G_{ref}.

We specified a hierarchical model for individual tree-level parameters in Equations 5 and 6 such that they vary around the associated species-level parameters, which accounts for individuals as random effects:

$$m_{t(i)} \sim \text{Normal}\left(\mu_{m_{s(t)}}, \sigma_m^2\right),$$

$$\alpha_{t(i)} \sim \text{Normal}\left(\mu_{\alpha_{s(t)}}, \sigma_\alpha^2\right), \quad (7)$$

$$\beta_{t(i)} \sim \text{Normal}\left(\mu_{\beta_{s(t)}}, \sigma_\beta^2\right),$$

where $s(t)$ indicates species s associated with tree t, and μ_m, μ_α and μ_β denote the species-level parameters. All remaining parameters were assigned relatively non-informative, standard priors (see Methods S1).

2.7 | Model implementation and interpretation

The above model (Equations 4–7) was implemented in JAGS 4.3.0 (Plummer, 2003) via the package 'RJAGS' (Plummer, 2013) in R 4.0.2 (R Core Team, 2020). Three parallel Markov chain Monte Carlo (MCMC)

chains were assigned dispersed initial values, run for 100,000 iterations and thinned by 100 for a total of 3,000 posterior samples. Convergence was verified with visual inspection and Gelman and Rubin's diagnostic (Gelman & Rubin, 1992). MCMC samples were summarized as a posterior mean and central 95% credible interval (CI). Parameters are significantly different from zero if the 95% CI did not contain zero. All data and code are hosted on GitHub (repository published upon accepted manuscript).

To evaluate sensitivity to D on the same scale across species, we calculated standardized stomatal sensitivity (S) as the ratio of m to G_{ref} following Oren, Sperry, et al. (1999). Because G_{ref} was modelled as a time-varying parameter related to CDE, S was calculated for each day n and species s:

$$S_{s,n} = \frac{\mu_{m_s}}{\left(\mu_{\alpha_s} + \mu_{\beta_s} \bullet \mathrm{CDE}_n\right)}, \quad (8)$$

wherein μ_m, μ_α and μ_β were obtained from the posterior MCMC samples. The resulting 3,000 samples of $S_{s,n}$ for each species and day were summarized as a posterior mean and central 95% CI, which allowed us to examine how species-level hydraulic regulation varied over time.

Plant hydraulic regulation exists along a continuum of iso/anisohydry (Klein, 2014; Martínez-Vilalta et al., 2014). Similarly, we use S as a continuous index of hydraulic regulation and consider $S \geq 0.6$ to be similar to mesic species (Oren, Sperry, et al., 1999) and representative of isohydric behaviour (Ogle et al., 2012), whereas $S < 0.6$ was considered relatively anisohydric.

3 | RESULTS

3.1 | Trends in D, water potential and sap flow

Across the elevation gradient, maximum daily D (D_{max}) and cumulative D exposure (CDE) were highest at the lowest elevation site, Jordan (Figure 2). Seasonal trends in CDE reveal that during June and July, CDE accumulated faster than later in the season, when D_{max} no longer consistently exceeded 1 kPa. Predawn water potentials (Ψ_{PD}) remained at or above −0.77 MPa for all species during the period of sap flux measurements (Figure S1). Midday water potentials (Ψ_{MD}) ranged from −1.27 MPa in the *Salix* hybrid to −2.50 MPa in *T. ramosissima* (Figure S1).

Except for *E. angustifolia*, sap flux density (J_s) varied between 20 and 50 g m^{-2} s^{-1}, with the highest elevation site having lower sap flux density (Figure 3). *E. angustifolia* had J_s values that were roughly one order of magnitude higher than the other species, including the ring-porous *T. ramosissima*. Species-specific coefficients were applied for both ring-porous species, which had smaller active sapwood depth relative to the total sensor length (Bush et al., 2010; Hultine, Nagler, et al., 2010).

3.2 | Model fit

The hierarchical model fit the observed canopy conductance (G_c) extremely well (Figure S3, observed vs. predicted G_c: $R^2 = 0.955$), with low bias (slope of observed vs. predicted = 0.953). When considered on a species-specific basis, R^2 of the model fit ranged from 0.589 (*P. fremontii*) to 0.900 (*Salix* hybrid, Figure S4), which supports our assumption that G_c approximates G_s.

3.3 | Covariate effects

Exploratory data analysis revealed that the G_c vs. log(D_{max}) relationship did not remain constant over the growing season. For multiple species, the intercept appeared to vary with day of year (Figure 4) and particularly with CDE (Figure S2). Therefore, rather than fitting a single linear relationship through all points, we hierarchically modelled reference conductance (G_{ref}, intercept of Oren model) as a linear function of CDE. We found that variation

FIGURE 2 Seasonal trends in cumulative vapour pressure deficit exposure (CDE, left axis, lines) and daily maximum vapour pressure deficit (D_{max}, right axis, points) at four study sites along an elevation gradient. Grey boxes indicate the sampling period at each site

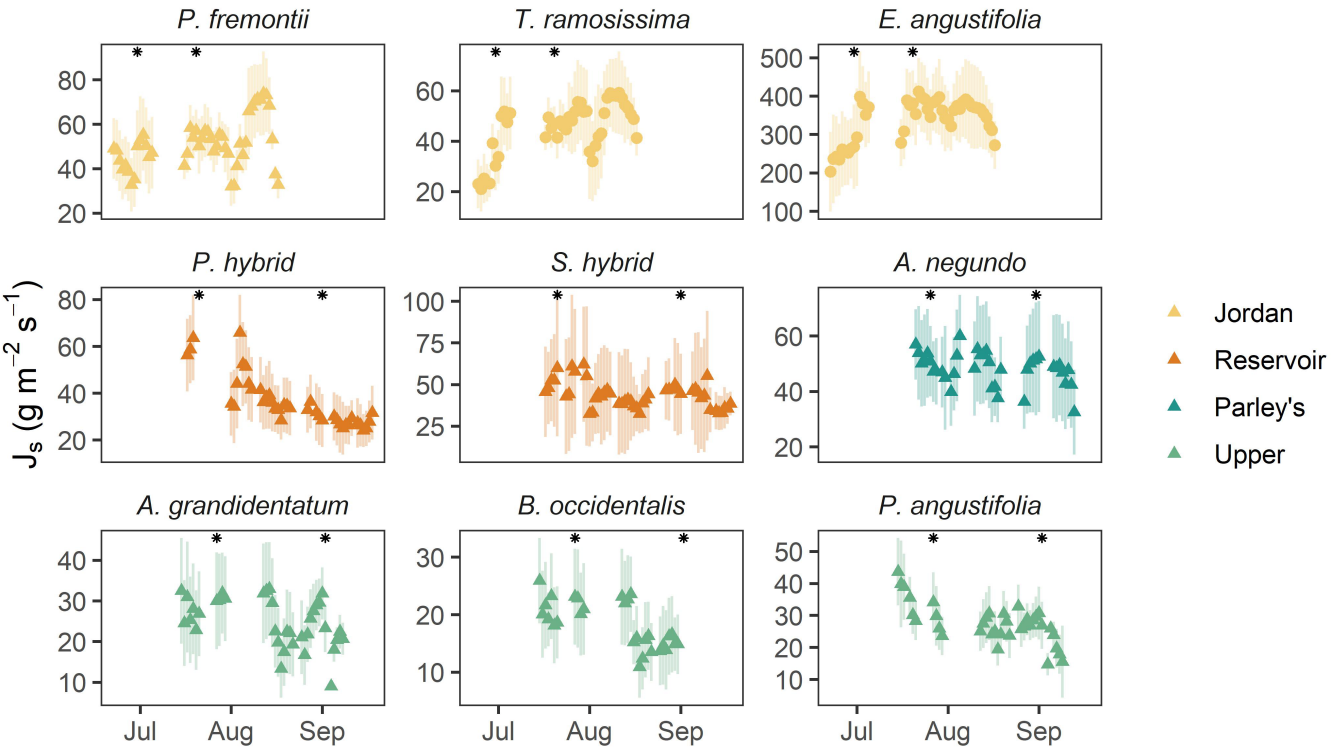

FIGURE 3 Seasonal trends in mean daytime sap flux density (J_s) for nine study species ($M \pm 1$ *SD*, see Table 1 for sample sizes). Only points for which there were at least three individual observations are shown. Triangles denote diffuse-porous, native species; circles denote ring-porous, non-native species; and asterisks denote dates when leaf water potentials were collected

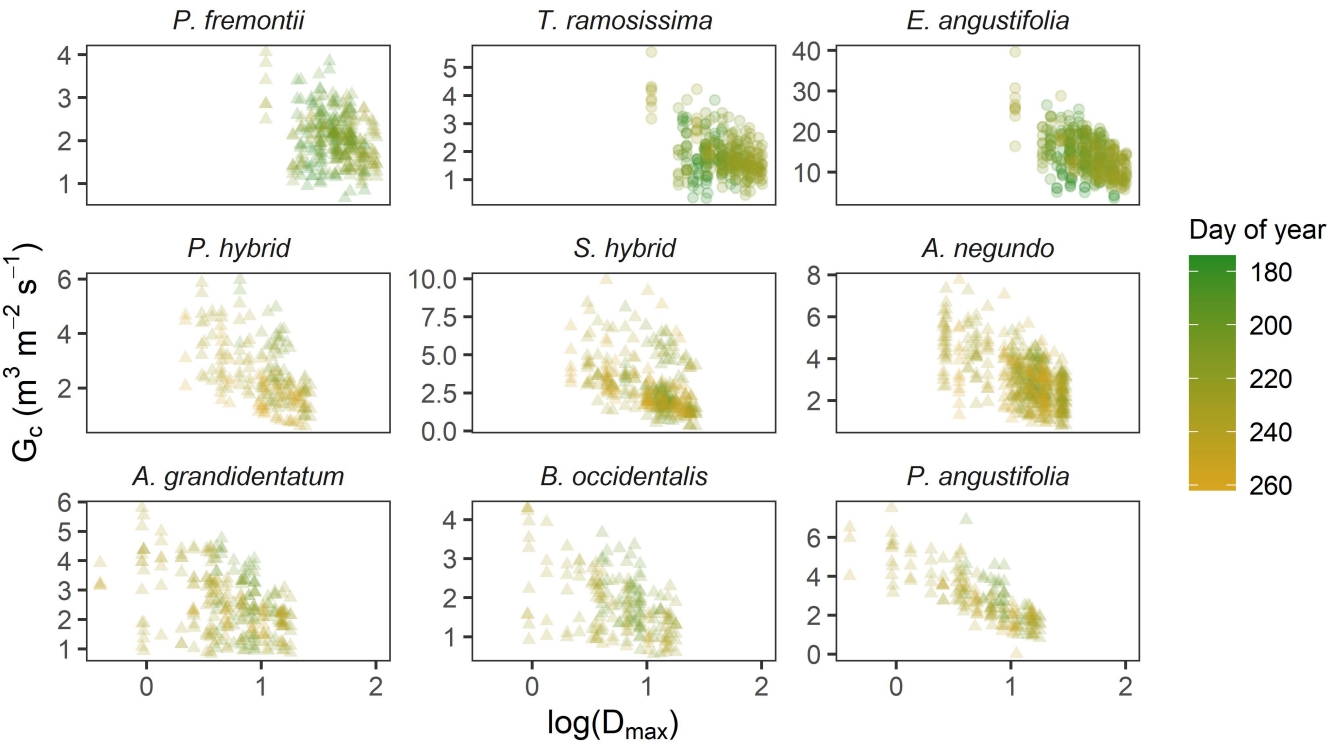

FIGURE 4 The relationship between mean daytime canopy conductance (G_c) and the natural log of D_{max} for nine study species. The colour axis represents the day of year. Triangles denote diffuse-porous, native species, and circles denote ring-porous, non-native species

in G_{ref} was significantly correlated with CDE in seven of nine species (Figure 5). For two ring-porous species at the low-elevation Jordan site (*T. ramosissima* and *E. angustifolia*), CDE exerted a positive influence on G_{ref}, such that G_{ref} increased during the growing season (Figure S5). However, for the remaining five species inhabiting mid to high elevations (Reservoir, Parley's and Upper sites), CDE was negatively associated with G_{ref}, which decreased during the growing season. *P. fremontii* at the Jordan site and *Salix* hybrid at the Reservoir site did not exhibit growing season variation in G_{ref} associated with CDE.

Across species, minimum Ψ_{MD} was not significantly correlated with the magnitude of the effect of CDE on G_{ref} (μ_β), although the two species with positive μ_β (*T. ramosissima* and *E. angustifolia*) also achieved the most negative minimum Ψ_{MD}.

3.4 | Stomatal sensitivity

Because standardized stomatal sensitivity (S) is inversely proportional to G_{ref} (Equation 8), the temporal patterns of S (Figure 6) are opposite to those of G_{ref} (Figure S5). *T. ramosissima* and *E. angustifolia* exhibited decreasing S over the growing season, even as all three species from the low-elevation Jordan site had low stomatal sensitivity throughout the season ($S < 0.6$). Five of six species at the three higher elevation sites exhibited increasing S across the growing season. *Populus* hybrid and *A. grandidentatum* transitioned from weakly anisohydric to isohydric ($S \geq 0.6$). Despite increasing S, *A. negundo* remained strongly anisohydric while *B. occidentalis* and *P. angustifolia*

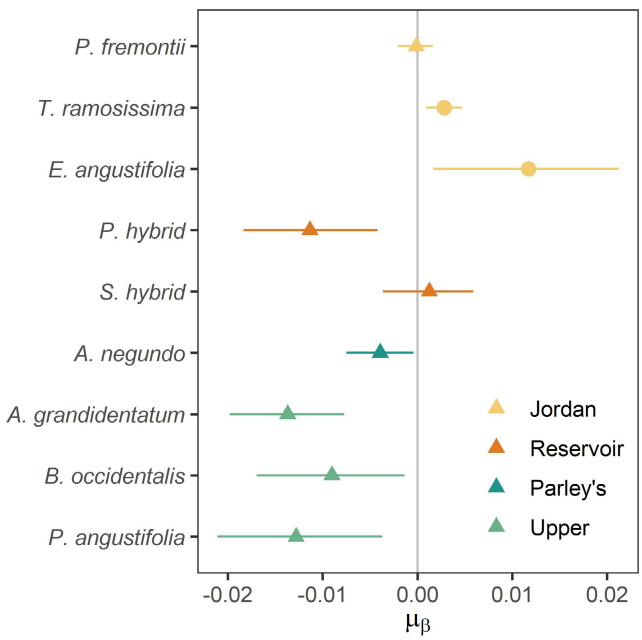

FIGURE 5 Species-level sensitivity of reference conductance (G_{ref}) to CDE (μ_β). Points represent the posterior mean, and error bars indicate the central 95% credible interval (CI). Triangles denote diffuse-porous, native species, and circles denote ring-porous, non-native species

stayed isohydric. The stomatal sensitivity of *P. fremontii* (Jordan) and *Salix* hybrid (Reservoir) did not change over time.

Among the three representatives of the genus *Populus*, low-elevation *P. fremontii* remained strongly anisohydric and the high-elevation *P. angustifolia* remained isohydric throughout the season, while the intermediate *Populus* hybrid more closely resembled *P. angustifolia*. Among the two *Acer* species, *A. negundo* was strongly anisohydric, in contrast to the more intermediate stomatal sensitivity of *A. grandidentatum* that shifted from weakly anisohydric to isohydric. Even among congeneric species, stomatal sensitivities and their temporal trends can strongly differ.

4 | DISCUSSION

Among nine dominant riparian tree species occurring along an elevation gradient, standardized stomatal sensitivity (S) was temporally variable across the growing season for seven species, driven by reference conductance that varied with cumulative D exposure. Temporal trends in S differed among the species, which reflected differences in exposure to cumulative D and wood anatomy. Despite the highest cumulative D at the low-elevation site, the two ring-porous species (*T. ramosissima* and *E. angustifolia*) exhibited decreasing stomatal sensitivity across the growing season (i.e. progressively more anisohydric). Among the three higher elevation sites, five diffuse-porous species experienced increasing S during the growing season, suggesting progressively more isohydric stomatal behaviour. We find that temporal shifts in hydraulic regulation can be driven by atmospheric moisture deficit, even in the absence of soil water limitations. Moreover, contrasts in temporal shifts in stomatal sensitivity, whereby non-native riparian tree taxa become progressively less sensitive relative to native taxa, may have important implications for future riparian forest community structure in the increasingly arid western United States.

4.1 | Temporal trends in stomatal sensitivity

Seasonal differences in plant hydraulic regulation have been reported across different metrics for characterizing hydraulic strategy. For example, the sensitivity of sap velocity to D differs between summer and winter in the evergreen gymnosperm *Callitris glaucophylla*, although not in the co-occurring evergreen angiosperm *Eucalyptus crebra* (Zeppel et al., 2004). From an index of iso/anisohydry quantified by the slope (σ) between predawn and midday Ψ (Martínez-Vilalta et al., 2014), seasonal shifts in plant hydraulic regulation have been previously reported in *Larrea tridentata* (Guo et al., 2020), *Quercus douglasii* (Feng et al., 2019) and *Quercus suber* (Haberstroh et al., 2021), all considered drought-tolerant species experiencing large variation in soil and atmospheric moisture conditions. In these species, stomatal sensitivity of individual plants decreases (i.e. became more anisohydric) during the wet season, consistent with prioritizing carbon gain while

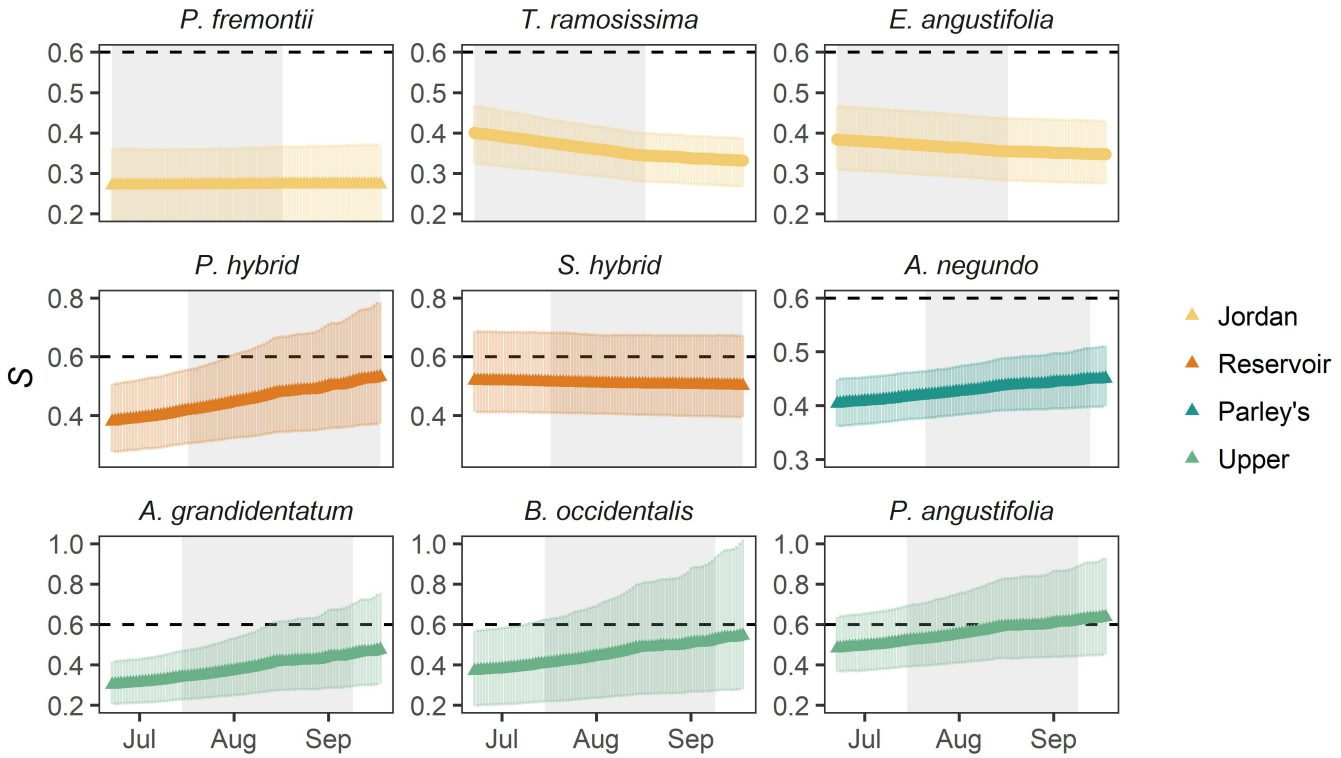

FIGURE 6 Predicted seasonal trends in standardized stomatal sensitivity ($S = m/G_{ref}$, sensu Oren, Sperry, et al., 1999). The dotted line at 0.6 indicates the S commonly found among mesic species (Oren, Sperry, et al., 1999). Points represent the posterior mean, and error bars indicate the central 95% credible interval (CI). Grey boxes indicate the sampling period at each site. Triangles denote diffuse-porous, native species, and circles denote ring-porous, non-native species. Note that y-axis scales are consistent for each site

conditions are amenable. However, in a meta-analysis of predawn and midday Ψ, the direction of change in σ from wet to dry years was species-specific (Wu et al., 2021). The potential contrasts between intra-annual versus inter-annual shifts in plant hydraulic regulation remain unresolved but could arise from differences in hydraulic traits and rainfall seasonality.

In this study, the nine Western riparian tree species were rooted near shallow water-tables, reflected by consistently high predawn water potentials (Figure S1). Thus, while Guo et al. (2020) showed that concomitant changes in D and soil moisture were associated with temporal shifts in σ, here we demonstrate that temporal shifts in hydraulic regulation can be driven by atmospheric moisture deficit alone, lending additional support to the importance of D for quantifying plant hydraulic regulation (Novick et al., 2019). We also found species-dependent changes in standardized stomatal sensitivity at the subannual scale, consistent with the findings of Wu et al. (2021) at the inter-annual scale. Future studies that incorporate multiple metrics of hydraulic regulation (reviewed in Feng et al., 2019) have the potential to reveal coordination, particularly between response- and trait-based metrics (Kannenberg et al., 2021).

4.2 | Potential traits underlying temporal shifts

Stomatal regulation mediates the impact of atmospheric demand on leaf water potential (Ψ_{leaf}), which is also influenced by hydraulic conductance between the soil and canopy. The ability of seven species to alter conductance at reference conditions (G_{ref}, Figure 5) suggests that individual plants often adjust hydraulic conductance across the growing season. For example, the ratio of water-supplying to water-demanding tissues can be altered by radial growth of new xylem (Fonti et al., 2010), root growth (Huang & Eissenstat, 2000) or embolism-induced loss of conductivity (Jaquish & Ewers, 2001; McCulloh et al., 2011). Similarly, leaf area changes via leaf abscission and regrowth (Dallstream & Piper, 2021; Filewod & Thomas, 2014) can change plant demand for water. Indeed, seasonal shifts in plant allometry can significantly impact hydraulic regulation, sometimes exceeding the influence of environmental variables (Kannenberg et al., 2021; Novick et al., 2019). Although allometric methods can be destructive and/or labour-intensive, repeated measurements of plant allometry within a season can shed additional light on variable hydraulic regulation.

At the whole-plant level, balance between water supply versus demand can be captured by the Huber value (Hv), or the ratio of sapwood area to leaf area (Tyree & Ewers, 1991). Increased Hv can reduce water potential gradients within plants and compensate for vulnerable xylem both across species (Mencuccini et al., 2019) and as a phenotypic response to increased aridity (López et al., 2016). Across species, Hv is negatively correlated with maximum xylem conductivity (Sanchez-Martinez et al., 2020) and reference conductance (Flo et al., 2021). If the inverse relationship holds true for individual trees over time, as it does in Australian species in four habitats

(McClenahan et al., 2004), we would expect the ring-porous species with increasing G_{sref} to decrease Hv over the season, with the opposite generally holding true for diffuse-porous species. However, repeated measurements of Hv are needed to confirm the mechanism driving increasing reference conductance in ring-porous species.

Ring- and diffuse-porous species exhibited contrasting seasonal trends in reference conductance: G_{ref} of ring-porous species increased with cumulative *D* exposure, while G_{ref} of diffuse-porous species either decreased or remained the same. At first glance, the idea of seasonally increasing G_{ref} in ring-porous species seems incongruous, as native hydraulic conductivity naturally decreases following the cavitation of earlywood vessels (Taneda & Sperry, 2008). However, in two *Quercus* species, the remaining small-diameter vessels can nonetheless sustain high rates of transpiration (Cochard & Tyree, 1990). Ring-porous species might sustain high conductivity using latewood vessels alone, whereas diffuse-porous species appear to suffer progressive loss of conductivity throughout the season (S. E. Bush et al., unpublished) and in response to drought (Hoffmann et al., 2011). Therefore, we posit that the progressive shift towards isohydry in diffuse-porous species can be attributed to the prevention of progressive embolism, while the progressive shift towards anisohydry in ring-porous species may reflect less vulnerable latewood vessels.

4.3 | Consequences for riparian trees and beyond

The dynamics of fluvial hydrology and groundwater availability undoubtedly act as strong agents of selection in riparian tree taxa in terms of rooting depth, hydraulic architecture, xylem anatomy and stomatal regulation. In general, riparian tree taxa are largely drought intolerant and have xylem that embolize at relatively high water potentials. For example, *A. negundo*, *B. occidentalis*, *P. angustifolia*, *P. fremontii*, *S. gooddingii* (a close relative of the *Salix* hybrid in the present study) and *T. ramosissima* have reported mean Ψ_{50} values that range between −1.29 and −1.61 MPa (Choat et al., 2012).

Broadly speaking, drought-intolerant species with higher (less negative) Ψ_{50} express greater regulation of leaf water potentials via stomatal conductance (i.e. more isohydric) (Skelton et al., 2015; Trifilò et al., 2015), suggesting that highly vulnerable riparian tree species should express strong isohydric patterns of stomatal regulation. However, three of the most vulnerable (highest Ψ_{50}) species in our synthesis displayed surprisingly insensitive ($S < 0.6$) stomatal responses to *D*, including *A. negundo*, *P. fremontii* and *T. ramosissima*. Likewise, *A. grandidentatum*, a species with a far more negative reported mean Ψ_{50} of −3.66 (Choat et al., 2012), also exhibited somewhat anisohydric behaviour early in the growing season. These results indicate that under well-watered conditions, stomatal sensitivity to *D* in some riparian taxa can be surprisingly low, particularly in warm-adapted taxa where leaf cooling may be prioritized over hydraulic safety (Aparecido et al., 2020; Blasini et al., 2022; Hultine et al., 2020).

The fact that the two ring-porous species in our survey were the only two species to demonstrate a positive correlation between G_{ref} and cumulative *D* (Figures 5 and 6) may have important implications for future tree community structure in western riparian forests because both species are invasive. Across 17 western states, *T. ramosissima* (and closely related *T. chinensis* and their hybrids) and *E. angustifolia* are currently the third and fourth most frequently occurring woody plants in the region, following only species of *Populus* and *Salix* (Friedman et al., 2005). Given the expressed decreased sensitivity of G_{ref} with cumulative *D*, it is plausible that a progressive increase in aridity across the western United States could further amplify the competitiveness of these two highly invasive tree species relative to native tree taxa, even where plant available soil water remains high. Conversely, species such as *A. grandidentatum*, *B. occidentalis* and *P. angustifolia* that generally occupy more mesic riparian habitats demonstrated strongly decreasing G_{ref} values with cumulative *D* (Figure 5), suggesting that increasing aridity could hasten the shrinking of these species' climate niche relative to other riparian tree taxa.

Importantly, the interpretation of results from the present study hinge on the assumption that stomatal regulation is constrained exclusively by *D*, and not limited by soil moisture. Predawn water potentials indicate that the trees were never exposed to significant soil water deficits, with mean values ranging from −0.77 MPa in *A. negundo* in September to −0.29 MPa in *P. fremontii* in July (Figure S1). Therefore, contrasts in seasonal variation of G_{ref} (and *S*) among species, we conclude, were primarily driven by species sensitivity to atmospheric aridity, quantified by stomatal responses to cumulative *D*. Given that changes in climate are bringing longer, more frequent and more intense heatwaves with higher *D* across the globe, riparian areas in arid regions are likely to experience profound changes in net primary productivity with potential changes in tree species assemblages. Furthermore, the impacts of higher *D* are likely not limited to riparian ecosystems, but should also impact other groundwater-dependent systems, and habitats where increasing atmospheric aridity is seasonally decoupled from soil water limitation, such as tropical or temperate regions.

5 | CONCLUSIONS

Even in the absence of soil moisture limitation, stomatal sensitivity of riparian tree taxa varies with respect to the cumulative effect of high *D* and differences in wood anatomy. Temporal changes in stomatal sensitivity were driven by changes in reference conductance, which reflects the balance between water-supplying and water-demanding tissues. Diffuse-porous species mostly experienced increasing stomatal sensitivity, a conservative hydraulic response which is consistent with accumulated xylem embolism. Interestingly, non-native ring-porous species were able to reduce stomatal sensitivity as the growing season progressed, which may reflect shifts towards greater safety in latewood vessels. While the mechanisms underlying seasonal variation in stomatal sensitivity are largely unknown, higher frequency measurement of hydraulic and allometric traits are needed to complement instrument data (e.g. sap flow,

stem psychrometers) to understand plant hydraulic regulation under novel climate conditions.

AUTHORS' CONTRIBUTIONS

J.S.G., S.E.B. and K.R.H. conceived the ideas; S.E.B. and K.R.H. collected the data; J.S.G. analysed the data; J.S.G. and K.R.H. led the writing of the manuscript. All authors contributed critically to the drafts and gave final approval for publication.

ACKNOWLEDGEMENTS

The authors thank Kelsey Bryant, Drew Peltier and Luiza Aparecido for their constructive feedback on earlier versions of the manuscript. Financial support was provided by a grant from the National Science Foundation's (Grant # 1340856) Macrosystems Biology program awarded to K.R.H. and a grant from the US Department of Agriculture, National Institute of Food and Agriculture (Grant #2015-67013-12138) awarded to K.R.H.

CONFLICT OF INTEREST

The authors declare no conflict of interest.

DATA AVAILABILITY STATEMENT

Data and code archived on Zenodo https://doi.org/10.5281/zenodo.6496555 (Guo et al., 2022).

ORCID

Jessica S. Guo https://orcid.org/0000-0002-9566-9182
Susan E. Bush https://orcid.org/0000-0002-0148-9157
Kevin R. Hultine https://orcid.org/0000-0001-9747-6037

REFERENCES

Aparecido, L. M. T., Woo, S., Suazo, C., Hultine, K. R., & Blonder, B. (2020). High water use in desert plants exposed to extreme heat. *Ecology Letters*, *23*, 1189–1200.

Aspinwall, M. J., King, J. S., Domec, J. C., McKeand, S. E., & Isik, F. (2011). Genetic effects on transpiration, canopy conductance, stomatal sensitivity to vapour pressure deficit, and cavitation resistance in loblolly pine. *Ecohydrology*, *4*, 168–182.

Blasini, D. E., Koepke, D. F., Bush, S. E., Allan, G. J., Gehring, C. A., Whitham, T. G., Day, T. A., & Hultine, K. R. (2022). Tradeoffs between leaf cooling and hydraulic safety in a dominant arid land riparian tree species. *Plant, Cell & Environment*. https://doi.org/10.1111/pce.14292

Brodribb, T. J., & McAdam, S. A. M. (2011). Passive origins of stomatal control in vascular plants. *Science*, *331*, 582–585.

Bush, S. E., Hultine, K. R., Sperry, J. S., & Ehleringer, J. R. (2010). Calibration of thermal dissipation sap flow probes for ring- and diffuse-porous trees. *Tree Physiology*, *30*, 1545–1554.

Choat, B., Jansen, S., Brodribb, T. J., Cochard, H., Delzon, S., Bhaskar, R., Bucci, S. J., Feild, T. S., Gleason, S. M., & Hacke, U. G. (2012). Global convergence in the vulnerability of forests to drought. *Nature*, *491*, 752–755.

Cochard, H., & Tyree, M. T. (1990). Xylem dysfunction in *Quercus*: Vessel sizes, tyloses, cavitation and seasonal changes in embolism. *Tree Physiology*, *6*, 393–407.

Dallstream, C., & Piper, F. I. (2021). Drought promotes early leaf abscission regardless of leaf habit but increases litter phosphorus losses only in evergreens. *Australian Journal of Botany*, *69*, 121–130.

Domec, J.-C., Noormets, A., King, J. S., Sun, G., McNulty, S. G., Gavazzi, M. J., Boggs, J. L., & Treasure, E. A. (2009). Decoupling the influence of leaf and root hydraulic conductances on stomatal conductance and its sensitivity to vapour pressure deficit as soil dries in a drained loblolly pine plantation. *Plant, Cell & Environment*, *32*, 980–991.

Doughty, C. E., & Goulden, M. L. (2008). Seasonal patterns of tropical forest leaf area index and CO_2 exchange. *Journal of Geophysical Research: Biogeosciences*, *113*, n/a–n/a.

Ewers, B. E., Mackay, D. S., & Samanta, S. (2007). Interannual consistency in canopy stomatal conductance control of leaf water potential across seven tree species. *Tree Physiology*, *27*, 11–24.

Feng, X., Ackerly, D. D., Dawson, T. E., Manzoni, S., McLaughlin, B., Skelton, R. P., Vico, G., Weitz, A. P., & Thompson, S. E. (2019). Beyond isohydricity: The role of environmental variability in determining plant drought responses. *Plant, Cell & Environment*, *42*, 1104–1111.

Filewod, B., & Thomas, S. C. (2014). Impacts of a spring heat wave on canopy processes in a northern hardwood forest. *Global Change Biology*, *20*, 360–371.

Flo, V., Martínez-Vilalta, J., Mencuccini, M., Granda, V., Anderegg, W. R. L., & Poyatos, R. (2021). Climate and functional traits jointly mediate tree water-use strategies. *New Phytologist*, *231*, 617–630.

Fonti, P., von Arx, G., García-González, I., Eilmann, B., Sass-Klaassen, U., Gärtner, H., & Eckstein, D. (2010). Studying global change through investigation of the plastic responses of xylem anatomy in tree rings. *New Phytologist*, *185*, 42–53.

Friedman, J. M., Auble, G. T., Shafroth, P. B., Scott, M. L., Merigliano, M. F., Freehling, M. D., & Griffin, E. R. (2005). Dominance of non-native riparian trees in western USA. *Biological Invasions*, *7*, 747–751.

Fu, X., & Meinzer, F. C. (2018). Metrics and proxies for stringency of regulation of plant water status (iso/anisohydry): A global data set reveals coordination and trade-offs among water transport traits. *Tree Physiology*, *39*, 122–134.

Gaskin, J. F., & Kazmer, D. J. (2009). Introgression between invasive saltcedars (*Tamarix chinensis* and *T. ramosissima*) in the USA. *Biological Invasions*, *11*, 1121–1130.

Gelman, A., & Rubin, D. B. (1992). Inference from iterative simulation using multiple sequences. *Statistical Science*, *7*, 457–472.

Granier, A. (1987). Evaluation of transpiration in a Douglas-fir stand by means of sap flow measurements. *Tree Physiology*, *3*, 309–320.

Grossiord, C., Buckley, T. N., Cernusak, L. A., Novick, K. A., Poulter, B., Siegwolf, R. T. W., Sperry, J. S., & McDowell, N. G. (2020). Plant responses to rising vapor pressure deficit. *New Phytologist*, *226*, 1550–1566.

Guo, J. S., Bush, S. E., & Hultine, K. R. (2022). Temporal variation in stomatal sensitivity to vapor pressure deficit in western riparian forests [data set]. *Zenodo*, https://doi.org/10.5281/zenodo.6496555

Guo, J. S., Hultine, K. R., Koch, G. W., Kropp, H., & Ogle, K. (2020). Temporal shifts in iso/anisohydry revealed from daily observations of plant water potential in a dominant desert shrub. *New Phytologist*, *225*, 713–726.

Haberstroh, S., Lobo-do-Vale, R., Caldeira, M., Dubbert, M., Cuntz, M., & Werner, C. (2021). *Plant invasion modifies isohydricity in Mediterranean tree species*. Authorea.

Hacke, U. G., Stiller, V., Sperry, J. S., Pittermann, J., & McCulloh, K. A. (2001). Cavitation fatigue. Embolism and refilling cycles can weaken the cavitation resistance of xylem. *Plant Physiology*, *125*, 779–786.

Hatfield, J. L., & Prueger, J. H. (2015). Temperature extremes: Effect on plant growth and development. *Weather and Climate Extremes*, *10*, 4–10.

Hoffmann, W. A., Marchin, R. M., Abit, P., & Lau, O. L. (2011). Hydraulic failure and tree dieback are associated with high wood density in a temperate forest under extreme drought. *Global Change Biology*, *17*, 2731–2742.

Horel, J., Splitt, M., Dunn, L., Pechmann, J., White, B., Ciliberti, C., Lazarus, S., Slemmer, J., Zaff, D., & Burks, J. (2002). Mesowest: Cooperative mesonets in the western United States. *Bulletin of the American Meteorological Society*, *83*, 211–226.

Huang, B., & Eissenstat, D. M. (2000). Linking hydraulic conductivity to anatomy in plants that vary in specific root length. *Journal of the American Society for Horticultural Science*, *125*, 260–264.

Hultine, K. R., Allan, G. J., Blasini, D., Bothwell, H. M., Cadmus, A., Cooper, H. F., Doughty, C. E., Gehring, C. A., Gitlin, A. R., Grady, K. C., Hull, J. B., Keith, A. R., Koepke, D. F., Markovchick, L., Corbin Parker, J. M., Sankey, T. T., & Whitham, T. G. (2020). Adaptive capacity in the foundation tree species *Populus fremontii*: Implications for resilience to climate change and non-native species invasion in the American southwest. *Conservation Physiology*, *8*(1), coaa061.

Hultine, K. R., Burtch, K. G., & Ehleringer, J. R. (2013). Gender specific patterns of carbon uptake and water use in a dominant riparian tree species exposed to a warming climate. *Global Change Biology*, *19*, 3390–3405.

Hultine, K. R., & Bush, S. E. (2011). Ecohydrological consequences of non-native riparian vegetation in the southwestern United States: A review from an ecophysiological perspective. *Water Resources Research*, *47*, W07542. https://doi.org/10.1029/2010WR010317

Hultine, K. R., Bush, S., & Ehleringer, J. (2010). Ecophysiology of riparian cottonwood and willow before, during, and after two years of soil water removal. *Ecological Applications*, *20*, 347–361.

Hultine, K. R., Bush, S. E., West, A. G., & Ehleringer, J. R. (2007). Effect of gender on sap-flux-scaled transpiration in a dominant riparian tree species: Box elder (*Acer negundo*). *Journal of Geophysical Research: Biogeosciences*, *112*, G03S06. https://doi.org/10.1029/2006JG000232

Hultine, K. R., Bush, S. E., West, A. G., Burtch, K. G., Pataki, D. E., & Ehleringer, J. R. (2008). Gender-specific patterns of aboveground allocation, canopy conductance and water use in a dominant riparian tree species: Acer negundo. *Tree Physiology*, *28*, 1383–1394.

Hultine, K. R., Nagler, P. L., Morino, K., Bush, S. E., Burtch, K. G., Dennison, P. E., Glenn, E. P., & Ehleringer, J. R. (2010). Sap flux-scaled transpiration by tamarisk (*Tamarix* spp.) before, during and after episodic defoliation by the saltcedar leaf beetle (*Diorhabda carinulata*). *Agricultural and Forest Meteorology*, *150*, 1467–1475.

Jaquish, L. L., & Ewers, F. W. (2001). Seasonal conductivity and embolism in the roots and stems of two clonal ring-porous trees, *Sassafras albidum* (Lauraceae) and *Rhus typhina* (Anacardiaceae). *American Journal of Botany*, *88*, 206–212.

Kannenberg, S. A., Guo, J. S., Novick, K. A., Anderegg, W. R. L., Feng, X., Kennedy, D., Konings, A. G., Martínez-Vilalta, J., & Matheny, A. M. (2021). Opportunities, challenges, and pitfalls in characterizing plant water-use strategies. *Functional Ecology*, *36*, 24–37.

Katul, G., Leuning, R., & Oren, R. (2003). Relationship between plant hydraulic and biochemical properties derived from a steady-state coupled water and carbon transport model. *Plant, Cell & Environment*, *26*, 339–350.

Klein, T. (2014). The variability of stomatal sensitivity to leaf water potential across tree species indicates a continuum between isohydric and anisohydric behaviours. *Functional Ecology*, *28*, 1313–1320.

López, R., Cano, F. J., Choat, B., Cochard, H., & Gil, L. (2016). Plasticity in vulnerability to cavitation of *Pinus canariensis* occurs only at the driest end of an aridity gradient. *Frontiers in Plant Science*, *7*, 769.

Martínez-Vilalta, J., Poyatos, R., Aguadé, D., Retana, J., & Mencuccini, M. (2014). A new look at water transport regulation in plants. *New Phytologist*, *204*, 105–115.

McAdam, S. A. M., Manzi, M., Ross, J. J., Brodribb, T. J., & Gómez-Cadenas, A. (2016). Uprooting an abscisic acid paradigm: Shoots are the primary source. *Plant Signaling & Behavior*, *11*, 6. https://doi.org/10.1080/15592324.2016.1169359

McClenahan, K., Macinnis-Ng, C., & Eamus, D. (2004). Hydraulic architecture and water relations of several species at diverse sites around Sydney. *Australian Journal of Botany*, *52*, 509–518.

McCulloh, K. A., Johnson, D. M., Meinzer, F. C., & Lachenbruch, B. (2011). An annual pattern of native embolism in upper branches of four tall conifer species. *American Journal of Botany*, *98*, 1007–1015.

McMaster, G. S., & Wilhelm, W. (1997). Growing degree-days: One equation, two interpretations. *Agricultural and Forest Meteorology*, *87*, 291–300.

McNaughton, K. G., & Jarvis, P. G. (1991). Effects of spatial scale on stomatal control of transpiration. *Agricultural and Forest Meteorology*, *54*, 279–302.

Mediavilla, S., & Escudero, A. (2003). Stomatal responses to drought at a Mediterranean site: A comparative study of co-occurring woody species differing in leaf longevity. *Tree Physiology*, *23*, 987–996.

Mencuccini, M., Rosas, T., Rowland, L., Choat, B., Cornelissen, H., Jansen, S., Kramer, K., Lapenis, A., Manzoni, S., & Niinemets, Ü. (2019). Leaf economics and plant hydraulics drive leaf: Wood area ratios. *New Phytologist*, *224*, 1544–1556.

Monteith, J. L., & Unsworth, M. H. (1990). *Principles of environmental physics* (2nd ed.). Edward Arnold.

Novick, K. A., Ficklin, D. L., Stoy, P. C., Williams, C. A., Bohrer, G., Oishi, A. C., Papuga, S. A., Blanken, P. D., Noormets, A., Sulman, B. N., Scott, R. L., Wang, L., & Phillips, R. P. (2016). The increasing importance of atmospheric demand for ecosystem water and carbon fluxes. *Nature Climate Change*, *6*, 1023–1027.

Novick, K. A., Konings, A. G., & Gentine, P. (2019). Beyond soil water potential: An expanded view on isohydricity including land–atmosphere interactions and phenology. *Plant, Cell & Environment*, *42*, 1802–1815.

Ogle, K., Lucas, R. W., Bentley, L. P., Cable, J. M., Barron-Gafford, G. A., Griffith, A., Ignace, D., Jenerette, G. D., Tyler, A., Huxman, T. E., Loik, M. E., Smith, S. D., & Tissue, D. T. (2012). Differential daytime and night-time stomatal behavior in plants from North American deserts. *New Phytologist*, *194*, 464–476.

Oren, R., Phillips, N., Ewers, B. E., Pataki, D. E., & Megonigal, J. P. (1999). Sap-flux-scaled transpiration responses to light, vapor pressure deficit, and leaf area reduction in a flooded Taxodium distichum forest. *Tree Physiology*, *19*, 337–347.

Oren, R., Sperry, J. S., Katul, G. G., Pataki, D. E., Ewers, B. E., Phillips, N., & Schäfer, K. V. R. (1999). Survey and synthesis of intra- and interspecific variation in stomatal sensitivity to vapour pressure deficit. *Plant, Cell & Environment*, *22*, 1515–1526.

Pantin, F., Monnet, F., Jannaud, D., Costa, J. M., Renaud, J., Muller, B., Simonneau, T., & Genty, B. (2013). The dual effect of abscisic acid on stomata. *New Phytologist*, *197*, 65–72.

Plummer, M. (2003). *JAGS: A program for analysis of Bayesian graphical models using Gibbs sampling*. Proceedings of the 3rd international workshop on distributed statistical computing, Vienna, Austria.

Plummer, M. (2013). *rjags: Bayesian graphical models using MCMC*. R package version, 3.

Poyatos, R., Granda, V., Flo, V., Adams, M. A., Adorján, B., Aguadé, D., Aidar, M. P. M., Allen, S., Alvarado-Barrientos, M. S., Anderson-Teixeira, K. J., Aparecido, L. M., Arain, M. A., Aranda, I., Asbjornsen, H., Baxter, R., Beamesderfer, E., Berry, Z. C., Berveiller, D., Blakely, B., … Martínez-Vilalta, J. (2021). Global transpiration data from sap flow measurements: The SAPFLUXNET database. *Earth System Science Data*, *13*, 2607–2649.

R Core Team. (2020). *R: A language and environment for statistical computing*. R Foundation for Statistical Computing.

Sanchez-Martinez, P., Martínez-Vilalta, J., Dexter, K. G., Segovia, R. A., & Mencuccini, M. (2020). Adaptation and coordinated evolution of plant hydraulic traits. *Ecology Letters*, *23*, 1599–1610.

Schäfer, K. V. R. (2011). Canopy stomatal conductance following drought, disturbance, and death in an upland oak/pine forest of the New Jersey Pine Barrens, USA. *Frontiers in Plant Science*, *2*, 15. https://doi.org/10.3389/fpls.2011.00015

Skelton, R. P., West, A. G., & Dawson, T. E. (2015). Predicting plant vulnerability to drought in biodiverse regions using functional traits. *Proceedings of the National Academy of Sciences of the United States of America*, *112*, 5744–5749.

Sperry, J., Hacke, U., Oren, R., & Comstock, J. (2002). Water deficits and hydraulic limits to leaf water supply. *Plant, Cell & Environment*, *25*, 251–263.

Sperry, J., Venturas, M. D., Anderegg, W. R., Mencuccini, M., Mackay, D. S., Wang, Y., & Love, D. M. (2017). Predicting stomatal responses to the environment from the optimization of photosynthetic gain and hydraulic cost. *Plant, Cell & Environment*, *40*, 816–830.

Taneda, H., & Sperry, J. S. (2008). A case-study of water transport in co-occurring ring-versus diffuse-porous trees: Contrasts in water-status, conducting capacity, cavitation and vessel refilling. *Tree Physiology*, *28*, 1641–1651.

Trifilò, P., Nardini, A., Gullo, M. A. L., Barbera, P. M., Savi, T., & Raimondo, F. (2015). Diurnal changes in embolism rate in nine dry forest trees: Relationships with species-specific xylem vulnerability, hydraulic strategy and wood traits. *Tree Physiology*, *35*, 694–705.

Tyree, M. T., & Ewers, F. W. (1991). The hydraulic architecture of trees and other woody plants. *New Phytologist*, *119*, 345–360.

Whitehead, D., & Jarvis, P. (1981). Coniferous forests and plantations. In T. Kozlowski (Ed.), *Water deficits and plant growth* (pp. 49–152). Academic Press.

Whitham, T. G., Bailey, J. K., Schweitzer, J. A., Shuster, S. M., Bangert, R. K., LeRoy, C. J., Lonsdorf, E. V., Allan, G. J., DiFazio, S. P., Potts, B. M., Fischer, D. G., Gehring, C. A., Lindroth, R. L., Marks, J. C., Hart, S. C., Wimp, G. M., & Wooley, S. C. (2006). A framework for community and ecosystem genetics: From genes to ecosystems. *Nature Reviews Genetics*, *7*, 510–523.

Wu, G., Guan, K., Li, Y., Novick, K. A., Feng, X., McDowell, N. G., Konings, A. G., Thompson, S. E., Kimball, J. S., & De Kauwe, M. G. (2021). Interannual variability of ecosystem iso/anisohydry is regulated by environmental dryness. *New Phytologist*, *229*, 2562–2575.

Yuan, W., Zheng, Y., Piao, S., Ciais, P., Lombardozzi, D., Wang, Y., Ryu, Y., Chen, G., Dong, W., Hu, Z., Jain, A. K., Jiang, C., Kato, E., Li, S., Lienert, S., Liu, S., Nabel, J. E. M. S., Qin, Z., Quine, T., … Yang, S. (2019). Increased atmospheric vapor pressure deficit reduces global vegetation growth. *Science Advances*, *5*, eaax1396.

Zeppel, M. J. B., Murray, B. R., Barton, C., & Eamus, D. (2004). Seasonal responses of xylem sap velocity to VPD and solar radiation during drought in a stand of native trees in temperate Australia. *Functional Plant Biology*, *31*, 461–470.

SUPPORTING INFORMATION

Additional supporting information may be found in the online version of the article at the publisher's website.

How to cite this article: Guo, J. S., Bush, S. E. & Hultine, K. R. (2022). Temporal variation in stomatal sensitivity to vapour pressure deficit in western riparian forests. *Functional Ecology*, *00*, 1–13. https://doi.org/10.1111/1365-2435.14066